Journal of
Composites Science

MDPI

Article

TiO_2@lipophilic Porphyrin Composites: New Insights into Tuning the Photoreduction of Cr(VI) to Cr(III) in Aqueous Phase

Antonio Pennetta [1,2], Sabrina Di Masi [3,*], Federica Piras [1], Xiangfei Lü [4], Jun Li [5], Giuseppe Edigio De Benedetto [2] and Giuseppe Mele [1]

1 Department of Engineering for Innovation, University of Salento, Via per Monteroni, 73100 Lecce, Italy; antonio.pennetta@unisalento.it (A.P.); federica.piras@unisalento.it (F.P.); giuseppe.mele@unisalento.it (G.M.)
2 Department of Cultural Heritages, University of Salento, Via per Monteroni, 73100 Lecce, Italy; giuseppe.debenedetto@unisalento.it
3 Department of Biological and Environmental Sciences and Technologies, University of Salento, Via per Monteroni, 73100 Lecce, Italy
4 School of Environmental Science and Engineering, Chang'An University, No. 126 Yanta Road, Xi'an 710054, China; lvxf@chd.edu.cn
5 College of Chemistry & Materials Science, Northwest University, 1 Xuefu Ave., Guodu, Chang'an District, Xi'an 710127, China; junli@nwu.edu.cn
* Correspondence: sabrina.dimasi@unisalento.it; Tel.: +39-0832-29-9457

Received: 4 June 2020; Accepted: 23 June 2020; Published: 26 June 2020

Abstract: Metal-free and Cu(II)-lipophilic porphyrins [H_2Pp and Cu(II)Pp] loaded on titanium dioxide in the anatase phase (TiO_2) were prepared and used as a heterogeneous catalyst for the photoreduction of Cr(VI) to Cr(III) in aqueous suspensions under UV–Vis light irradiation. TiO_2 impregnated with copper(II) porphyrin [TiO_2@Cu(II)Pp] was the most effective in photocatalyst reduction of toxic chromate Cr(VI) to non-toxic chromium Cr(III). We further evaluated an experimental design with the scope of fast optimization of the process conditions related to the use of TiO_2 or TiO_2-porphyrin based photocatalysts. A full factorial design as a chemometric tool was successfully employed for screening the affecting factors involved in photoconversion catalysis, with the modification of TiO_2 both with porphyrin H_2Pp and Cu(II)Pp. The studied experimental factors were the catalyst amount, the concentration of Cr(VI) ions, and the pH of the medium. The performed multivariate approach was successfully used for fast fitting and better evaluation of significant factors affecting the experimental responses, with the advantage of reducing the number of available experiments. Thus, the stability of the optimized TiO_2 embedded Cu(II)Pp was investigated, confirming the high reproducibility and suitability for environmental purposes.

Keywords: titanium dioxide; catalyst; porphyrin; photocatalytical reduction; Cr(VI) ions; experimental design

1. Introduction

Heavy metals represent a cause of environmental contamination that affects the quality of the different matrices, thus, monitoring is nowadays strictly required. Even in trace concentrations, heavy metals can accumulate at different levels in trophic pathways and the toxicity of specific metal ions is largely known. The species of metal ions usually monitored because of their toxicity are also explicated at trace concentrations such as Hg, Cd, Pb, As, and Cr. Generally, the common persistent species of chromium present in the environment are represented by the trivalent and hexavalent form (Cr(III) and Cr(VI), respectively). Basically, Cr(III) is relatively non-toxic and can be found in trace amounts as

an essential nutrient in various biological pathways, whereas Cr(VI) is related to highly toxic effects on health and the environment [1]. Chemically, the chromate species are strong oxidants and act as carcinogens, mutagens, and teratogens. Considering the use of hexavalent chromium in dyeing, wood, textile, metallurgy, and tanning industries and its toxic nature, the development of an eco-friendly and low-cost process to remove Cr(VI) from sensitive stores is a great challenge for the wastewater and process waste industries [2].

Currently, the most commonly employed processes for the removal of Cr(VI) are adsorption, biosorption [3,4], electrocoagulation, ion exchange, reverse osmosis, liquid–liquid extraction, precipitation, photocatalytical reduction [5,6], and electrochemistry [7,8]. In particular, the photocatalytical reduction of chromate ions mostly employs titanium dioxide (TiO_2) as the catalyst [3,5,9–13]. Basically, the photocatalysis of TiO_2 structures mainly hinges on the excitations of electrons from the semiconductor's valence band (VB) to the conduction band (CB), which are thus involved in redox processes. The photogenerated electrons are also responsible for the highly reductive properties of photocatalyst reactions [14]. Moreover, the advantages of using TiO_2 as photocatalysts include the lower synthesis cost, eco-friendly application, and their photo resistance, which reveal their suitability as composite materials for different purposes.

Titanium dioxide catalysts opportunely sensitized with lipophilic porphyrins or phthalocyanines have been particularly used both in the degradation of organic compounds [15] and in photoreduction reactions of CO_2 to formic acid [16]. Additionally, the application of TiO_2 and Cu/TiO_2 structures for the photoreduction of CO_2 to methanol has been reported in the literature [17]. Enzyme modified TiO_2 has also been studied for efficient and clean photoreduction to CO under visible light [18]. Furthermore, in order to improve the photocatalytic performances of TiO_2, dyes and pigments as impregnated nanomaterials have been successfully proposed. For example, dye-sensitized TiO_2 has been applied for solar energy conversion, photocatalysis, and related processes, with the advantage of involving low cost technologies, decreasing the negative impact on the environment and enhancing power conversion at the same time. Porphyrins are among the most interesting sensitizers capable of enhancing the photocatalytic activity of TiO_2 in the visible light region [15,19,20]. In fact, the presence of porphyrin structures increased the photocatalytic reactions due to the position and spacer length of peripherally substituted groups on porphyrin, the strength of the other involved polar groups, and the electroactivity of the atoms [20]. Recently, among these sensitizers, various Cu(II) porphyrins–TiO_2 have been proposed for the photodegradation of organics [21,22] and hydrogen production [23]. In light of these considerations, the possibility of promoting light induced photocatalysis can be considered as a promising approach for the fabrication of novel composites with unique physical-chemical properties with the scope to transform Cr(VI) to Cr(III) in water matrices [24].

With the aim to remove toxic compounds from the environment, an effective green method is highly desirable. In this respect, the favorable operation conditions of photocatalyst composites represent a promising and alternative approach for practical applications when compared with conventional methods. In light of this, this work relies on the application of our previously prepared catalyst [25] impregnated with a renewable and natural *meso*-tetraarylporphyrin with metal-free and metal complexes (with Cu^{2+}) for the photocatalyst reduction of Cr(VI) ions. From the application point of view, the stability of catalysts plays an important role and their performances can be faster evaluated by using condensed methods. The investigation of catalyst performances most commonly follows the univariate one-factor-at-time (OFAT) approach, where parameters are subsequently treated and screened as independent of each other. In contrast, multivariate evaluation of parameters by design of experiments (DOE) offers a statistically significant model of a phenomenon by performing a minimum set of experiments [26,27]. The advantage consists of obtaining a model suited for describing the importance of each variable and the interaction effects between them. Moreover, the multivariate analysis allows for the reduction in cost and time of operation processes, which is highly required for real contexts.

In this work, TiO_2 powders were impregnated with a lipophilic metal-free porphyrin [H_2Pp] and copper porphyrin [Cu(II)Pp], respectively, according to a procedure developed by Mele and co-workers [12]. To the best of our knowledge, this is the first time that the composites, listed as TiO_2@Cu(II)Pp and TiO_2@H_2Pp, have been used as heterogeneous catalysts for the photoreduction of Cr(VI) to Cr(III) in aqueous suspensions under UV–Vis light irradiation, and their activity was compared with the pristine TiO_2. We successfully adopted a DOE as a key-tool to assess and quickly compare the performances of the TiO_2, TiO_2@H_2Pp, and TiO_2@Cu(II)Pp composites. Thus, the effects of (i) pH, (ii) Cr(VI) ion concentration, and (iii) catalyst amount were simultaneously investigated with respect to the photoreduction efficiency of Cr(VI) to Cr(III) ions under UV–Vis light. The experimental design was successfully applied for faster evaluation of the performances of these kinds of catalysts. Upon the selected conditions, the reproducibility and reusability of the catalysts were studied and finally proposed for the photoreduction of Cr(VI) ions in water suspension.

2. Materials and Methods

2.1. Chemicals

Titanium dioxide of a high degree of purity in the crystalline form of anatase (specific surface area 8 m^2 g^{-1}) was provided by Huntsman Tioxide (Varese, Italy). H_2SO_4 (98%), $CuCl_2$, $K_2Cr_2O_7$, and 1,5-diphenylacarbazide were purchased from Sigma-Aldrich (Milano, Italy). Ultrapure water (Millipore System) was used as the solvent. The porphyrins employed in this work, opportunely functionalized with lipophilic (3-(pentadeca-8-enyl)-phenol) chains derived of a natural origin, were prepared for the first time as previously reported [25]. H_2Pp and Cu(II)Pp were successively impregnated onto the TiO_2 surface and the related composites TiO_2@H_2Pp and TiO_2@Cu(II)Pp were produced according to the previously described procedure [12]. All other chemicals used in this work were of analytical grade and were used without any purification.

2.2. Photocatalytic Activity

The photocatalytic activity of different catalysts (TiO_2, TiO_2@H_2Pp and TiO_2@Cu(II)Pp) were investigated by observing the efficiency of the photocatalytic conversion of Cr(VI) ions in water. Briefly, the experimental setup consisted of a batch photoreactor containing 50 mL of the catalyst dispersion and a solution of Cr(VI) in water. The mixture was magnetically stirred at 1000 rpm and irradiated using a Osram UltraVitalux UV-Vis lamp (OSRAM, Milano, Italy) at the distance of 15 cm from the batch solution. The emission spectrum of the lamp is shown in Figure 1.

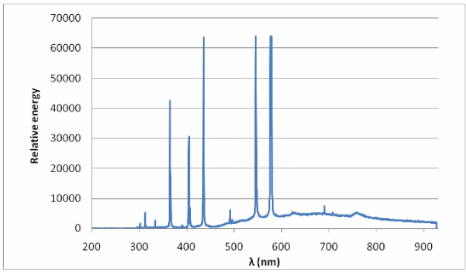

Figure 1. Emission spectrum of Osram UltraVitalux UV-Vis lamp.

During the photoreaction, samples (1 mL) were taken out at specific time intervals (15, 30, and 60 min) and filtered to remove the catalyst dispersion. The residual concentration of Cr(VI) ions in solution was determined by using the UV–Vis spectrophotometer with the standardized colorimetric method of 1,5-diphenyl carbazide (DPC, λ = 540 nm) [28]. The photoreduction efficiency (PE) of the catalysts was estimated from Equation (1):

$$PE\ (\%) = (C_0 - C_t)/C_0 \times 100 \quad (1)$$

where C_0 and C_t were the initial concentration and the residual concentration at the irradiation time t, respectively. A schematic diagram of the experimental setup is presented in Scheme 1.

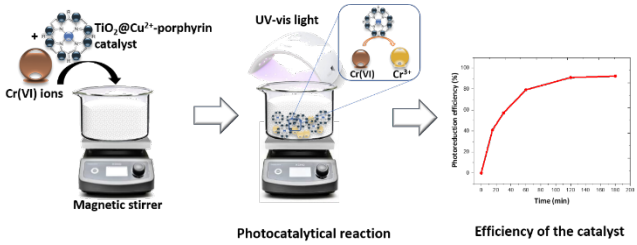

Scheme 1. Schematic diagram for the adopted experimental setup and analytical responses obtained for the conversion of Cr(V) ions by using TiO_2 or TiO_2-porphyrin based photocatalysts.

2.3. Experimental Design

Multivariate analysis was conducted to investigate the variables on the photoreduction efficiency and covered all interactions between parameters. Basically, the experimental design was a full factorial, with three replicated central points (2^k, k = 3; central points: 3). The pH, Cr(VI) concentration, and the amount of catalyst were selected as variables. A total of 11 experiments were conducted randomly to avoid the occurrence of unwanted systematic effects. The responses of the unmodified catalyst (TiO_2), the TiO_2@H_2Pp, and the TiO_2@Cu(II)Pp were compared and all the results were analyzed using MODDE 12.1 software (Umetrics, Umea, Sweden). The selected factors were studied in two levels, as reported in Table 1.

Table 1. Levels of factor.

Factors	Units	Low	High
pH (X_1)	-	2	5
[Cr(VI)] (X_2)	mg L^{-1}	5	15
Catalyst amount (X_3)	mg L^{-1}	500	1500

As previously reported by our group [16], the optimized ratio between Cu(II)Pp and TiO_2 composite was found to be 6.65 µmol/g per TiO_2 and thus selected for further investigation. The level of each factor agreed with those reported in the literature. In particular, the levels of pH were chosen according to the observed enhanced catalytical efficiency of TiO_2 at lower pH [29]. A solution of sulfuric acid (0.1 N) was used to bring the desiderated pH within 2 and 5. The concentration of Cr(VI) and the amount of catalyst were studied in the range between 5–15 mg L^{-1} and 500–1500 mg L^{-1}, respectively. The polynomial equation for 2^3 factors containing coefficients weighting both linear terms and their interactions is reported in Equation (2):

$$Y = b_0 + b_1X_1 + b_2X_2 + b_3X_3 + b_{12}X_1X_2 + b_{13}X_1X_3 + b_{23}X_2X_3 + b_{123}X_1X_2X_3 \quad (2)$$

where b_0, b_i, and b_{ij} represent the coefficient related to the constant, linear, and interaction terms, respectively.

2.4. Raman Spectroscopy Characterization

The Micro-Raman measurements were carried out with a Renishaw inVia instrument, equipped with two laser sources, a diode and a He–Cd laser with excitation wavelengths of 785 nm and 442 nm, respectively, edge filters for both laser lines, and a Leica DMLM microscope [30,31] (Leica, Solms, Germany) with motorized xyz stage and objectives up to 50x with a spatial resolution of about 2 µm. Neutral density filters were employed to keep the laser power at a low level (0.5–2 mW) on the samples to avoid undesired heating effects. The spectra were collected with repeated acquisitions (3–5)

each of 10 s. The wavelength scale was calibrated using a Si(111) standard (520.5 cm^{-1}). The catalyst, the porphyrin structures, and the modified catalyst free metal and metal chelated one were compared, and the obtained spectra were identified with that reported in the literature.

3. Results and Discussion

3.1. Full Factorial Design

In this work, the multivariate analysis conducted by MODDE software permitted us to elucidate (i) the distribution of the experimental data; (ii) the significance of factors; and (iii) the model fitting the experimental values, confirmed by the reproducibility and validity of the model. Table 2 shows the experimental matrix and the relative responses (Y, photoreduction efficiency) in the case of TiO_2, TiO_2@H_2Pp, and TiO_2@Cu(II)Pp, respectively.

Table 2. Experimental model matrix obtained for the TiO_2, TiO_2@H_2Pp, and TiO_2@CuPp catalysts. Responses were collected after 60 min of irradiation.

Exp No	Run Order	pH	Cr(VI), mg L^{-1}	Catalyst, mg L^{-1}	Photoreduction Efficiency, %		
					TiO_2	TiO_2@H_2Pp	TiO_2@CuPp
1	1	2	5	500	37	37	41
2	7	5	5	500	21	18	23
3	6	2	15	500	17	16	31
4	5	5	15	500	12	14	16
5	4	2	5	1500	41	67	88
6	9	5	5	1500	38	28	48
7	2	2	15	1500	47	28	50
8	8	5	15	1500	17	15	22
9	3	3.5	10	1000	25	23	28
10	10	3.5	10	1000	27	28	32
11	11	3.5	10	1000	29	30	30

As a preliminary note, the TiO_2@Cu(II)Pp catalyst had the highest photoconversion efficiency compared to the others. In particular, experiment no. 5 showed the highest achieved differences in photoreduction efficiency, whereas slight photocatalytical activity was observed in the other cases. Under the experimental conditions of experiment no. 5, TiO_2@Cu(II)Pp revealed the maximum photoreduction efficiency of Cr(VI), as expected. In fact, the increased activity can be easily ascribed to the presence of metal porphyrin, which leads to the enhanced electron transport into TiO_2 networks. In fact, we have already demonstrated that the presence of copper into the coordination of macrocycles plays a favorable role in photoreaction processes [15]. The mechanism for the enhanced photoactivity of TiO_2@Cu(II)Pp is schematically described in Scheme 2.

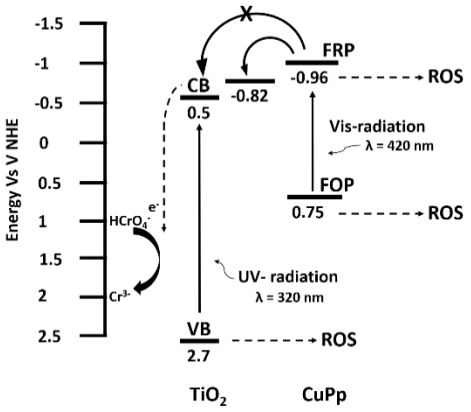

Scheme 2. Mechanism of electron transport of the catalyst in the presence of CuPp.

As described in Scheme 2, the higher performances of TiO_2 in the presence of Cu(II)Pp is due to the electron and hole transfer between the catalyst structures. In particular, Cu–Pp caused the edge shift responsible for the electron transport [23]. In the presence of UV light irradiation, the photogenerated electrons can be attracted by Cu(II)Pp, leading to the lower charge recombination. In addition, the photoinduced electrons of Cu(II)Pp are transferred to the conduction band of TiO_2, confirming the synergic effects between the catalyst and the proposed metal chelated porphyrin. Therefore, in the presence of visible light, the improvement of photocatalytical effect is mainly due to the presence of Cu(II)Pp.

3.1.1. Distribution of Experimental Data

Figure 2 shows the distribution of row experimental points (green points) and the replicates at the central point (blue points).

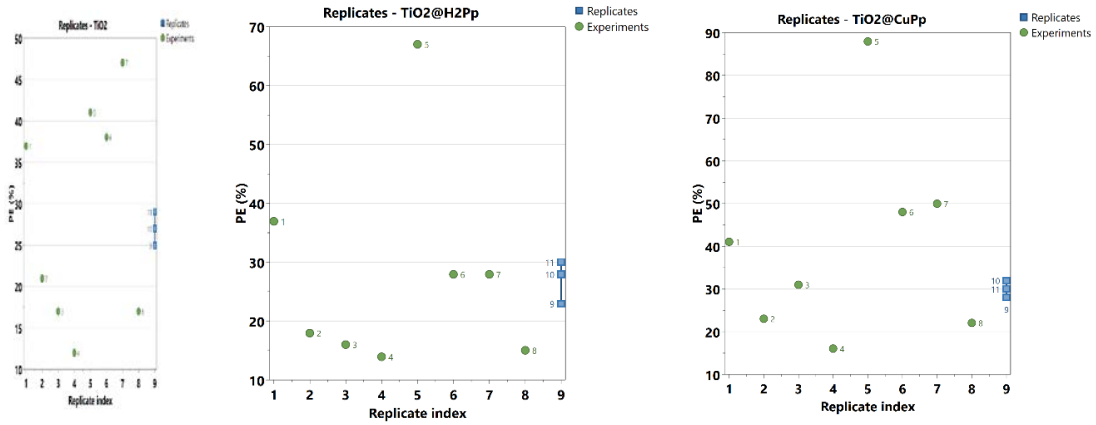

(**a**) (**b**) (**c**)

Figure 2. Replicate plots obtained for (**a**) TiO_2, (**b**) TiO_2@H_2Pp, and (**c**) TiO_2@Cu(II)Pp catalysts.

The variability of the collected experimental data was higher than that obtained in the case of the replicated points. The high reproducibility of the system in the whole experimental domain was demonstrated by the low variability of the response at central points. Non-normality of data distribution required a normalization by a logarithmic transformation.

3.1.2. Significance of Factors (Coefficients)

The normalized responses were modeled based on Equation (2) and significant coefficients were plotted in Figure 3.

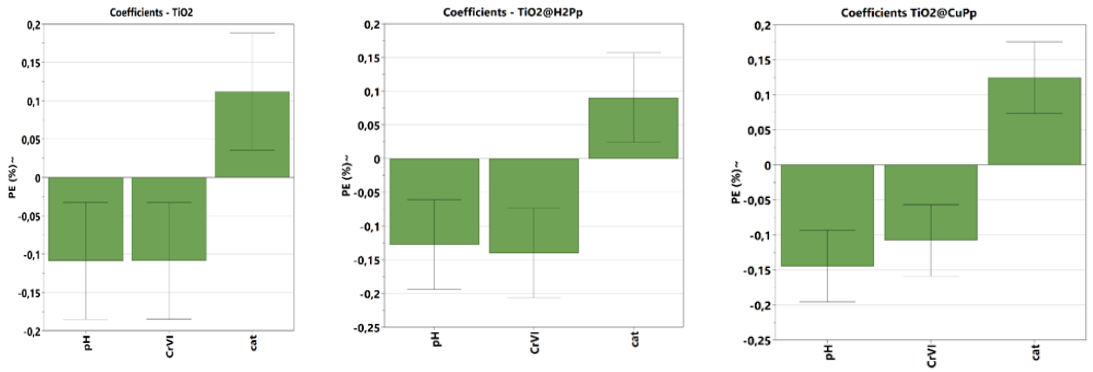

(**a**) (**b**) (**c**)

Figure 3. Plots of the significant coefficients obtained for (**a**) TiO_2, (**b**) TiO_2@H_2Pp, and (**c**) TiO_2@Cu(II)Pp catalysts.

The regression equations for normalized responses were obtained in the case of using TiO_2, TiO_2@H_2Pp, and TiO_2@Cu(II)Pp catalysts:

$$\log PE_{TiO2} = 1.41 - 0.10X_1 - 0.10X_2 + 0.11\ X_3 \quad (3)$$

$$\log PE_{H2PpTiO2} = 1.39 - 0.12\ X_1 - 0.14\ X_2 + 0.09\ X_3 \quad (4)$$

$$\log PE_{Cu(II)PpTiO2} = 1.52 - 0.14X_1 - 0.10X_2 + 0.12\ X_3 \quad (5)$$

where X_1, X_2,and X_3 were the pH, the Cr(V) concentration, and the amount of catalyst, respectively. It was found that the significant coefficients were linked to the linear terms of the three studied factors. As a result of Equations (3)–(5), the weight of coefficients related to pH and the concentration of Cr(VI) was negative, as expected. This means that the lower levels of pH and concentration of Cr(VI) allowed for higher photocatalytic conversion. Moreover, the pH of the solution strictly induces modifications of the surface properties of the catalyst, also influencing the ionic forms of chromium [32–34]. Normally, the electrostatic interactions between the hydroxyl groups of TiO_2 and Cr(VI) occur under acidic conditions (pH around 2 or 3) [35]. At pH = 2.5, chromate ions are present as $HCrO_4^-$, CrO_4^{2-}, or $Cr_2O_7^{2-}$ ions, whereas the active sites of the catalyst are highly protonated, leading Cr(VI) species to adsorb onto the surface of the catalysts via an electrostatic interaction [35]. Alternatively, at high pH, the surface of the catalyst becomes negative, with the subsequent repulsion of $Cr_2O_7^{2-}$ ions, reducing the photocatalytical efficiency [36].

It has also been reported that the high concentration of Cr(VI) generally blocks the activity of the catalyst, decreasing the interaction with the functional groups on the catalyst. Alternatively, the catalyst showed high catalytical conversion at any concentration below 5 mg/L; therefore, the concentration of Cr(VI) ions was investigated below those values. On the other hand, the amount of catalyst positively affected the efficiency of the photocatalytic reaction because of the higher specific surface area of the catalyst. However, an excessive concentration of the catalyst might induce particle aggregation [37] with a loss of overall performance.

3.1.3. Plots of Residual

The estimation of residuals is reported in Figure 4.

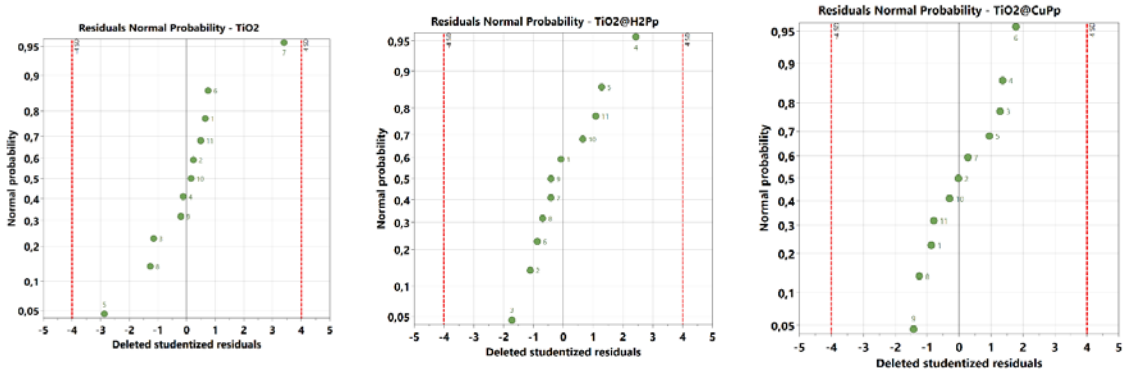

(**a**) (**b**) (**c**)

Figure 4. Plot of residuals obtained for the (**a**) TiO_2, (**b**) TiO_2@H_2Pp, and (**c**) TiO_2@Cu(II)Pp catalysts.

The results show that the residuals were normally distributed and the points on the probability plot followed close to a straight line. In addition, these results confirmed the great quality of the model, allowing it to be easily used to perform the screening of significant factors by reducing the number of experiments.

3.1.4. Summary of Fit

Figure 5 clearly shows the validity and reproducibility of the proposed mathematical model. The evaluated parameters elucidating the goodness of the model and its practicability to screen and predict the efficiency of chemical reactions were the R^2, Q^2, model validity, and the reproducibility. R^2 is the ability of the model in fitting row data variability, while Q^2 describes the ability of the model to predict the responses. Higher values of R^2 and Q^2 are substantially related to the goodness of the model. As shown in Figure 5, the selected mathematical model could explain the overall variability of the studied reaction, confirmed by the high correlated values of R^2, Q^2, and the reproducibility around the three investigated central points (Figure 5). As also reported in this latter case, the mathematical model was able to predict the overall behavior of the catalytical reaction by highlighting the importance to consider all the interactions existing between factors.

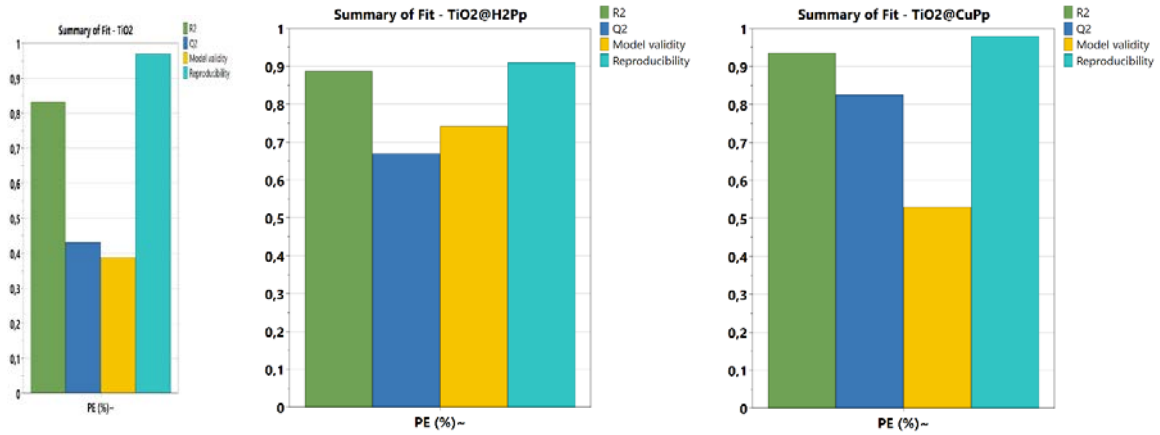

(**a**) (**b**) (**c**)

Figure 5. Summary plots obtained for (**a**) TiO_2, (**b**) TiO_2@H_2Pp, and (**c**) TiO_2@Cu(II)Pp catalysts. Parameters are shown as follows: R^2: green bar; Q^2: blue bar; Model validity: yellow bar; Reproducibility: light blue bar.

Additionally, it appears that the prediction and validity of the model toward the experimental data were higher than that reported for the responses collected on TiO_2 catalyst. As these parameters were directly correlated to the overall variability observed between the experimental results, it seems that the functionalization of porphyrin on the TiO_2 structure positively influences the efficiency of the catalyst activity.

3.1.5. Design of Experiments (DOE) through the Time of Irradiation

The experimental data collected at 15 and 30 minutes of irradiation were additionally analyzed by MODDE software. Results for the TiO_2 catalyst showed no effect of factors on the achieved responses in both the tested aliquots. In addition, the validity and reproducibility of the model appeared to be poor. In the case of the TiO_2@H_2Pp catalyst, the studied factors affected the response when the photocatalytical reaction reached 30 minutes. The further modification of the nanocomposite with Cu^{2+} ions improved the photocatalytical efficiency of the catalyst. In fact, indicators like residual distribution, significant factors, and R^2 were high, indicating that the optimal photocatalytic conversion could be achieved after the modification of the catalyst with metal chelated porphyrin.

3.2. Raman Spectroscopy

Figure 6 shows the Raman spectra recorded for TiO_2, H_2Pp, TiO_2@H_2Pp, and TiO_2@Cu(II)Pp, respectively. The spectra are reported as acquired and were not baseline subtracted.

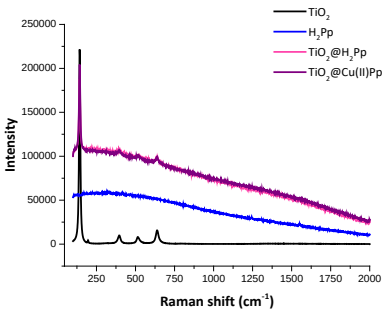

Figure 6. Raman spectra of TiO_2, H_2Pp, TiO_2@H_2Pp, and TiO_2@Cu(II)Pp catalysts.

The observed Raman frequencies for the bare TiO_2 structure were 144, 192, 395, 515, and 635 cm^{-1}, as reported in the literature in the case of anatase [38]. When the substrate was treated with either H_2Pp or Cu(II)Pp, the intensity of these peaks was clearly reduced, whereas the onset of a fluorescence background was observed. This is good evidence, although indirect, of the adsorption of H_2Pp or Cu(II)Pp on the TiO_2 catalyst. The same spectra were recorded on TiO_2@Cu(II)Pp after the catalytic experiments.

3.3. Stability of TiO_2@Cu(II)Pp Nanocomposite

Reusability of a photocatalyst is one of the most important keys in catalysis research for its utilization to be cost effective and practical. Our optimized catalyst may be promising for Cr(VI) removal from wastewater. The major sources of Cr(VI) include chemical industrial processes, plastic products, manufacturers of pharmaceuticals, and so on, which contribute to the emission of Cr(VI) in wastewater matrices in the concentration range between 0.1 and 200 mg L^{-1}. Moreover, the catalyst can also be proposed for underground water monitoring of Cr(VI) thanks to its operation in a more environmentally-friendly pH (nearby 5), which appears particularly favorable in obtaining higher retentions of chromium complex in abyssal water (pH = 6) [39]. Accordingly, the further re-usage measurements were conducted by selecting 1500 mg L^{-1} of catalyst and 1 mg L^{-1} as the initial concentration of Cr(VI) at pH = 5. Therefore, the stability of the TiO_2@Cu(II)Pp catalyst was evaluated by measuring the photocatalytical efficiency after six repeated cycles of measurements over 180 min of reaction time (Figure 7a,b).

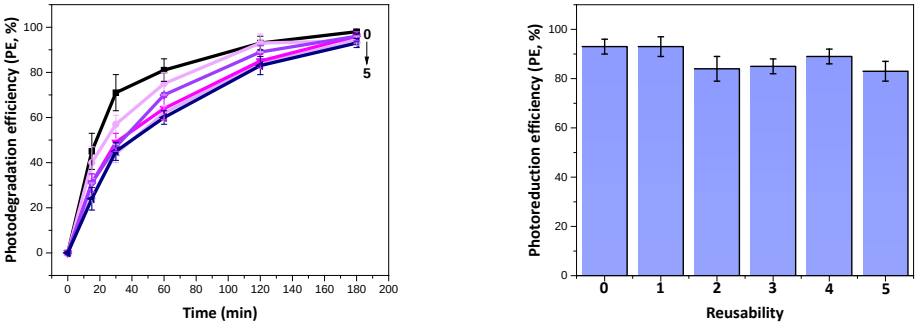

(**a**) (**b**)

Figure 7. Stability tests (**a,b**) performed for TiO_2@Cu(II)Pp catalyst after (0) the fresh preparation, (1) one, (2) two, (3) three (4) four, and (5) five reusage.

Photocatalytic efficiency as a function of time is presented in Figure 7a. The results show the increase in photocatalytic efficiency from 0 to 180 min of reaction time. The only slight decrease in photocatalytic efficiency was noticeable after five repetitive measurements, which revealed the high reliability of the proposed composite. Moreover, after 120 min of reaction time, the photocatalysis

reached maximus percentage in all cases. Figure 7 also confirms the observed high reproducibility of the TiO_2@Cu(II)Pp catalyst, revealing it as promising for future environmental applications.

4. Conclusions

In this work, a multivariate experimental design was adopted to perform the screening of affecting variables on the photocatalytical conversion of Cr(VI) in water by the TiO_2@Cu(II)Pp catalyst. The approach was successfully used to avoid the high number of experiments needed to perform a univariate operative work. Additionally, the experimental design allowed us to identify all the significant factors to be considered in the optimization processes, based on an accurate statistical analysis. The proposed model was also able to describe the physics of the processes and its statistical validation allowed us to predict the responses under defined conditions. As a result, the catalyst's efficiency of conversion was maximized by Cu(II) ion-based composite materials. Finally, the synergy between porphyrins and titanium dioxide in photocatalytic reactions and their flexibility also demonstrated their effectiveness for real-practical Cr(VI) reduction in polluted water matrices.

Author Contributions: Conceptualization, A.P. and S.D.M.; Methodology, A.P.; Software, A.P.; Validation, A.P. and S.D.M; Formal analysis, A.P., F.P., J.L., and X.L.; Data curation, A.P., F.P., S.D.M., J.L., and X.L.; Synthesis of porphyrins, X.L.; Preparation of TiO_2@Pp composites, A.P.; Writing—original draft preparation, A.P. and S.D.M.; writing—review and editing, G.E.D.B. and G.M.; Supervision, S.D.M., G.E.D.B., and G.M. All authors have read and agreed to the published version of the manuscript.

Funding: The authors thank the projects SAFEA: High-End Foreign Experts Project (Program No. GDW20186100251 and No. G20190027043), Programma Operativo Nazionale Ricerca e Innovazione 2014–2020 (CCI 2014IT16M2OP005), and Fondo Sociale Europeo, Azione I.1 "Dottorati Innovativi con caratterizzazione Industriale (DOT1312707)" for their financial support.

Conflicts of Interest: The authors declare no conflicts of interest.

References

1. Moretto, A. Hexavalent and trivalent chromium in leather: What should be done? *Regul. Toxicol. Pharmacol.* **2015**, *73*, 681–686. [CrossRef]
2. Dhal, B.; Thatoi, H.N.; Das, N.N.; Pandey, B.D. Chemical and microbial remediation of hexavalent chromium from contaminated soil and mining/metallurgical solid waste: A review. *J. Hazard. Mater.* **2013**, *250–251*, 272–291. [CrossRef]
3. Zhao, Y.; Chang, W.; Huang, Z.; Feng, X.; Ma, L.; Qi, X.; Li, Z. Enhanced removal of toxic Cr(VI) in tannery wastewater by photoelectrocatalysis with synthetic TiO_2 hollow spheres. *Appl. Surf. Sci.* **2017**, *405*, 102–110. [CrossRef]
4. Thatoi, H.; Das, S.; Mishra, J.; Rath, B.P.; Das, N. Bacterial chromate reductase, a potential enzyme for bioremediation of hexavalent chromium: A review. *J. Environ. Manag.* **2014**, *146*, 383–399. [CrossRef]
5. Yang, Y.; Yan, L.; Li, J.; Li, J.; Yan, T.; Sun, M.; Pei, Z. Synergistic adsorption and photocatalytic reduction of Cr(VI) using Zn-Al-layered double hydroxide and TiO_2 composites. *Appl. Surf. Sci.* **2019**, *492*, 487–496. [CrossRef]
6. Prabavathi, S.L.; Kumar, P.S.; Saravanakumar, K.; Muthuraj, V.; Karuthapandian, S. A novel sulphur decorated 1-D MoO_3 nanorods: Facile synthesis and high performance for photocatalytic reduction of hexavalent chromium. *J. Photochem. Photobiol. A Chem.* **2018**, *356*, 642–651. [CrossRef]
7. Vellaichamy, B.; Periakaruppan, P.; Nagulan, B. A novel sulphur decorated 1-D MoO_3 nanorods: Facile synthesis and high performance for photocatalytic reduction of hexavalent chromium. *ACS Sustain. Chem. Eng.* **2017**, *5*, 9313–9324. [CrossRef]
8. Barrera-Díaz, C.E.; Lugo-Lugo, V.; Bilyeu, B. A review of chemical, electrochemical and biological methods for aqueous Cr(VI) reduction. *J. Hazard. Mater.* **2012**, *223–224*, 1–12. [CrossRef]
9. Athanasekou, C.; Romanos, G.E.; Papageorgiou, S.K.; Manolis, G.K.; Katsaros, F.; Falaras, P. Photocatalytic degradation of hexavalent chromium emerging contaminant via advanced titanium dioxide nanostructures. *Chem. Eng. J.* **2017**, *318*, 171–180. [CrossRef]

10. Sanad, M.M.S.; Abdel-Aal, E.A.; Osman, H.M.; Kandil, A.T. Photocatalytic reduction of hexavalent chromium with commercial Fe/Ti oxide catalyst under UV and visible light irradiation. *Int. J. Environ. Sci. Technol.* **2018**, *15*, 2459–2472. [CrossRef]
11. Li, Y.; Bian, Y.; Qin, H.; Zhang, Y.; Bian, Z. Photocatalytic reduction behavior of hexavalent chromium on hydroxyl modified titanium dioxide. *Appl. Catal. B Environ.* **2017**, *206*, 293–299. [CrossRef]
12. Mele, G.; Del Sole, R.; Vasapollo, G.; Garcìa-Lòpez, E.; Palmisano, L.; Mazzetto, S.E.; Attanasi, O.A.; Filippone, P. Polycrystalline TiO_2 impregnated with cardanol-based porphyrins for the photocatalytic degradation of 4-nitrophenol. *Green Chem.* **2004**, *6*, 604–608. [CrossRef]
13. Mohapatra, P.; Samantaray, S.K.; Parida, K. Photocatalytic reduction of hexavalent chromium in aqueous solution over sulphate modified titania. *J. Photochem. Photobiol. A Chem.* **2005**, *170*, 189–194. [CrossRef]
14. Chen, D.; Ray, A.K. Removal of toxic metal ions from wastewater by semiconductor photocatalysis. *Chem. Eng. Sci.* **2001**, *56*, 1561–1570. [CrossRef]
15. Mele, G.; Del Sole, R.; Vasapollo, G.; García-López, E.; Palmisano, L.; Schiavello, M. Photocatalytic degradation of 4-nitrophenol in aqueous suspension by using polycrystalline TiO_2 impregnated with functionalized Cu(II)-porphyrin or Cu(II)-phthalocyanine. *J. Catal.* **2003**, *217*, 334–342. [CrossRef]
16. Mele, G.; Annese, C.; D'Accolti, L.; De Riccardis, A.; Fusco, C.; Palmisano, L.; Scarlino, A.; Vasapollo, G. Photoreduction of carbon dioxide to formic acid in aqueous suspension: A comparison between phthalocyanine/TiO_2 and porphyrin/TiO_2 catalysed processes. *Molecules* **2015**, *20*, 396–415. [CrossRef]
17. Wu, J.C.S.; Lin, H.M. Photo reduction of CO_2 to methanol via TiO_2 photocatalyst. *Int. J. Photoenergy* **2005**, *7*, 115–119. [CrossRef]
18. Woolerton, T.W.; Sheard, S.; Reisner, E.; Pierce, E.; Ragsdale, S.W.; Armstrong, F.A. Efficient and clean photoreduction of CO_2 to CO by enzyme-modified TiO_2 nanoparticles using visible light. *J. Am. Chem. Soc.* **2010**, *132*, 2132–2133. [CrossRef]
19. Zhao, X.; Wang, Y.; Feng, W.; Lei, H.; Li, J. Enhanced removal of toxic Cr(VI) in tannery wastewater by photoelectrocatalysis with synthetic TiO_2 hollow spheres. *RSC Adv.* **2017**, *7*, 52738–52746. [CrossRef]
20. Wang, C.; Li, J.; Mele, G.; Duan, M.Y.; Fei Lü, X.; Palmisano, L.; Vasapollo, G.; Zhang, F.X. The photocatalytic activity of novel, substituted porphyrin/TiO_2-based composites. *Dyes Pigments* **2010**, *84*, 183–189. [CrossRef]
21. Wang, L.; Jin, P.; Huang, J.; She, H.; Wang, Q. Integration of Copper(II)-Porphyrin Zirconium Metal-Organic Framework and Titanium Dioxide to Construct Z-Scheme System for Highly Improved Photocatalytic CO_2 Reduction. *ACS Sustain. Chem. Eng.* **2019**, *7*, 15660–15670. [CrossRef]
22. Gholamrezapor, E.; Eslami, A. Sensitization of magnetic TiO_2 with copper(II) tetrahydroxylphenyl porphyrin for photodegradation of methylene blue by visible LED light. *J. Mater. Sci. Mater. Electron.* **2019**, *30*, 4705–4715. [CrossRef]
23. Guo, X.; Li, X.; Qin, L.; Kang, S.Z.; Li, G. A highly active nano-micro hybrid derived from Cu-bridged TiO_2/porphyrin for enhanced photocatalytic hydrogen production. *Appl. Catal. B Environ.* **2019**, *243*, 1–9. [CrossRef]
24. Bhati, A.; Anand, S.R.; Saini, D.; Gunture Sonkar, S.K. Sunlight-induced photoreduction of Cr(VI) to Cr(III) in wastewater by nitrogen-phosphorus-doped carbon dot. *SNPJ Clean Water* **2019**, *2*, 1–9. [CrossRef]
25. Attanasi, O.A.; Del Sole, R.; Filippone, P.; Mazzetto, S.E.; Mele, G.; Vasapollo, G. Synthesis of novel lipophilic porphyrin-cardanol derivatives. *J. Porphyr. Phthalocyanines* **2004**, *8*, 1276–1284. [CrossRef]
26. Bezerra, M.A.; Lemos, V.A.; Novaes, C.G.; de Jesus, R.M.; Filho, H.R.S.; Araújo, S.A.; Alves, J.P.S. Application of mixture design in analytical chemistry. *Microchem. J.* **2020**, *152*, 104336. [CrossRef]
27. De Benedetto, G.E.; Di Masi, S.; Pennetta, A.; Malitesta, C. Response surface methodology for the optimisation of electrochemical biosensors for heavy metals detection. *Biosensors* **2019**, *9*, 26. [CrossRef]
28. EPA. *Method 7196A (Chromoium Hexavalent, Colorimetric)*; EPA: Washington, DC, USA, 1992; pp. 5–6.
29. Ku, Y.; Jung, I.L. Photocatalytic reduction of Cr(VI) in aqueous solutions by UV irradiation with the presence of titanium dioxide. *Water Res.* **2001**, *35*, 135–142. [CrossRef]
30. Fico, D.; Pennetta, A.; Rella, G.; Savino, A.; Terlizzi, V.; De Benedetto, G.E. A combined analytical approach applied to Medieval wall paintings from Puglia (Italy): The study of painting techniques and its conservation state. *J. Raman Spectrosc.* **2016**, *47*, 321–328. [CrossRef]
31. van der Werf, I.D.; Fico, D.; De Benedetto, G.E.; Sabbatini, L. The molecular composition of Sicilian amber. *Microchem. J.* **2016**, *125*, 85–96. [CrossRef]

32. Fang, S.; Zhou, Y.; Zhou, M.; Li, Z.; Xu, S.; Yao, C. Facile synthesis of novel $ZnFe_2O_4$/CdS nanorods composites and its efficient photocatalytic reduction of Cr(VI) under visible-light irradiation. *J. Ind. Eng. Chem.* **2018**, *58*, 64–73. [CrossRef]
33. Kim, W.; Park, J.Y.; Kim, Y. Fabrication of branched-TiO_2 microrods on the FTO glass for photocatalytic reduction of Cr(VI) under visible-light irradiation. *J. Ind. Eng. Chem.* **2019**, *73*, 248–253. [CrossRef]
34. Naimi-Joubani, M.; Shirzad-Siboni, M.; Yang, J.K.; Gholami, M.; Farzadkia, M. Photocatalytic reduction of hexavalent chromium with illuminated ZnO/TiO_2 composite. *J. Ind. Eng. Chem.* **2015**, *22*, 317–323. [CrossRef]
35. Jiang, F.; Zheng, Z.; Xu, Z.; Zheng, S.; Guo, Z.; Chen, L. Aqueous Cr(VI) photoreduction catalyzed by TiO_2 and sulfated TiO_2. *J. Hazard. Mater.* **2006**, *134*, 94–103. [CrossRef] [PubMed]
36. Padhi, D.K.; Parida, K. Facile fabrication of α-FeOOH nanorod/RGO composite: A robust photocatalyst for reduction of Cr(vi) under visible light irradiation. *J. Mater. Chem. A* **2014**, *2*, 10300–10312. [CrossRef]
37. Yang, Y.; Zhang, H.; Wang, P.; Zheng, Q.; Li, J. The influence of nano-sized TiO_2 fillers on the morphologies and properties of PSF UF membrane. *J. Membrane Sci.* **2007**, *288*, 231–238. [CrossRef]
38. Stagi, L.; Carbonaro, C.M.; Corpino, R.; Chiriu, D.; Ricci, P.C. Light induced TiO_2 phase transformation: Correlation with luminescent surface defects. *Phys. Status Solidi Basic Res.* **2015**, *252*, 124–129. [CrossRef]
39. Bohdziewicz, J. Removal of chromium ions (VI) from underground water in the hybrid complexation-ultrafiltration process. *Desalination* **2000**, *129*, 227–235. [CrossRef]